Soft Matter

PAPER

View Article Online
View Journal | View Issue

Cite this: *Soft Matter*, 2015, 11, 7165

Field induced anisotropic cooperativity in a magnetic colloidal glass

E. Wandersman,*[ab] Y. Chushkin,[c] E. Dubois,[a] V. Dupuis,[a] A. Robert[d] and R. Perzynski[a]

Received 28th May 2015,
Accepted 3rd August 2015

DOI: 10.1039/c5sm01315a

www.rsc.org/softmatter

The translational dynamics of a repulsive colloidal glass-former is probed by time-resolved X-ray Photon Correlation Spectroscopy. In this dense dispersion of charge-stabilized and magnetic nanoparticles, the interaction potential can be tuned, from quasi-isotropic to anisotropic by applying an external magnetic field. This powerful control parameter finely tunes the anisotropy of the intricate energy landscape in the colloidal glass-former, which is seen here as a new tunable model-system to probe the dynamical heterogeneities at the approach of the glass transition. Both structural and dynamical anisotropies are reported on interparticle lengthscales associated with highly anisotropic cooperativity, almost two orders of magnitude larger in the field direction than in the perpendicular direction and in zero field.

1 Introduction

In many disordered systems, the transition from the fluid to the solid state remains puzzling: when decreasing the temperature, or increasing the density, the dynamics slows down by several orders of magnitude, whereas ensemble-averaged static structural properties are weakly affected. This abrupt slowing-down, referred to as the glass transition, is observed in numerous disordered systems,[1,2] from frustrated magnets, to molecular and colloidal glasses and granular systems. It is widely accepted that the divergence of the relaxation time is accompanied by a growing length scale resulting in dynamical heterogeneities.[3–6] The structural relaxations occur through cooperative rearrangements of clusters of mobile particles. The size of these dynamically correlated clusters is evaluated by the dynamical susceptibilities χ_4.[5,7] For hard-sphere systems, the Mode Coupling Theory (MCT) predicts scaling laws,[5,6] both for the divergence of the relaxation time and χ_4.

Many experimental works are therefore conducted to extract the size of dynamically heterogeneous regions. In molecular and magnetic systems, its measurement is delicate and requires an indirect evaluation through non-linear response measurements.[8–11] An increase of χ_4 is observed as temperature is lowered. In colloidal systems, experiments using confocal microscopy[4,12] or scattering techniques[13,14] provide an easier access to space and time resolved dynamics, and thus to χ_4. In ref. 6 the growth of χ_4 with the packing fraction Φ in colloidal hard sphere glasses is observed. χ_4 diverges at $\Phi \approx 64\%$, but MCT predictions do not fit the data over the whole Φ range. However, fine variations and determinations of Φ are difficult to perform experimentally in concentrated samples and require many independent experiments. In addition, the relevance of such an averaged macroscopic quantity to characterize the nature of local structural relaxations is questionable.[15] An external parameter allowing to perturb the local structure at constant Φ while measuring its dynamical response would be of great interest experimentally.

Precisely to unravel the relationship between the local structure, dynamics and mechanical properties, many numerical and experimental studies have considered dynamical properties under shear.[16–18] At low shear rate ($\dot{\gamma} < \tau_r^{-1}$, where τ_r is the structural relaxation time), Chikkadi *et al.* report long-range spatial correlations in the fluctuations of microscopic strain associated with an anisotropic angular distribution. This anisotropy tends to disappear at higher shear rates. Beside the macroscopic shear studies, some recent works used a micro-rheological approach[19–21] to perturb locally the system. In ref. 21 the authors consider a single particle driven by a constant force in a glass-forming system. Beyond the linear response regime, an anomalous – superdiffusive – dynamics takes place in the parallel direction to the force, while it remains diffusive in the perpendicular direction. Interestingly, this superdiffusive anisotropic dynamics is associated with wide tails in the distribution of displacements. These features are in agreement with biased trap models[22] that consider the dynamics of a particle in an anisotropic free energy landscape. Experimental measurements

[a] Sorbonne Universités, UPMC Univ Paris 06, UMR 8234, Laboratoire PHENIX - CNRS - UPMC - ESPCI, Boîte 51, 4 place Jussieu, F-75005, Paris, France. E-mail: elie.wandersman@upmc.fr
[b] Sorbonne Universités, UPMC Univ Paris 06, UMR 8237, Laboratoire Jean Perrin, CNRS - UPMC, Boîte 114, 4 place Jussieu, F-75005, Paris, France
[c] European Synchrotron Radiation Facility - 6 rue J. Horowitz BP 220, 38043, Grenoble, Cedex 9, France. E-mail: chushkin@esrf.fr
[d] SLAC National Accelerator Laboratory, Linac Coherent Light Source, 2575 Sand Hill Rd, Menlo Park, CA 94025, USA

of χ_4 would help to understand these anomalous dynamics in biased energy landscapes or in driven systems.

In this paper, we report experiments on a colloidal glass based on magnetic nanoparticles and we study the effect of an external magnetic field on both its structural and dynamical properties. We show that the application of a magnetic field allows to tune and orient the cooperativity of the dynamics. We discuss these effects considering the fluctuations induced by local magnetization inhomogeneities along the field direction as an external source of energy. The perturbation of the dynamics by an external field appears as a powerfull tool to study dynamical heterogeneities at the approach of the glass transition.

2 Material and methods

The investigated system is a repulsive colloidal glass consisting of charged nanoparticles (NP) of maghemite (diameter $d \approx 10$ nm) dispersed in water. The interparticle repulsion due to the surface charge of these particles dominates and can be tuned with the ionic strength. The glassy sample is prepared from a fluid using an osmotic stress technique.[23] This allows to set the ionic strength and to increase Φ slowly enough to control the state of interaction of the system.[24] Each NP is also a nanomagnet with a magnetic moment $\mu \sim 10^4\ \mu_B$. In absence of magnetic field **H**, the magnetic moments of the NPs are randomly oriented. The magnetic dipolar interaction contribution, attractive on average, remains small ($U_{dd} \sim 0.7\ k_BT$) with respect to the electrostatic repulsion ($U_{elec} \sim 10\ k_BT$). The interaction potential is dominated by electrostatic repulsion[25] and in good approximation isotropic. We report here on systems similars to those of ref. 26 which display slow dynamics and aging above $\Phi = 25\%$.

The translational dynamics is probed using X-ray Photon Correlation Spectroscopy (XPCS) at the ID10C beamline of the ESRF (Grenoble, France). The energy of the partially coherent incident beam ($40 \times 40\ \mu m^2$) is set to 7.03 keV to minimize sample absorption. The coherently scattered X-rays form speckle patterns on a CCD detector (Princeton Instrument), located 3.3 m from the sample. In this configuration, the accessible wavevectors ($0.02 < Q < 0.05\ Å^{-1}$) covers the interparticle lengthscales. A speckle pattern is collected every 8 to 15 s to get sufficient statistics. A more precise measure of the static structure (with complementary Small Angle X-ray Scattering, SAXS) is performed at the ID02 beamline of the ESRF at 12 keV. Both experiments are performed with and without an applied field. A thin sample layer ($\sim$100 μm) is deposited on the wall of a quartz capillary, previously filled with dodecane to avoid water evaporation during the experiment. The sample age t_w is initiated as the capillary is placed in measuring conditions and no more subjected to any external mechanical stress. To apply the external permanent magnetic field **H** (320 kA m^{-1} corresponding to 90% of dipole alignment), a set of magnets is added to the setup, perpendicularly to the beam direction, in the horizontal plane. They are removed for **H** = 0 experiments. Note that the colloidal dispersion remains monophasic in presence of a magnetic field.[23] Last, under-field the scattering pattern is anisotropic. The intensity is thus analyzed over angular sectors of 20 degrees both along or perpendicularly to **H** direction.

3 Static structure

We investigate the dynamics of a sample with a volume fraction $\Phi = 30\%$. It is a freshly prepared glass-former[27] chosen for its slow dynamics, lying in the accessible time window of XPCS. We do not observe any noticeable evolution of its static structure on this time window. The structure factor $S(Q)$ without field (Fig. 1) determined by SAXS is characteristic of repulsive interactions, with a low compressibility of 0.04 and a mean interparticle distance of $\sim$12 nm. Each NP can be seen as an effective sphere of diameter $d + 2\kappa^{-1} \approx 12.5$ nm, where d is the diameter of the NP and $\kappa^{-1} \approx 1.2$ nm, the effective screening length of the potential. This latter is evaluated by adjusting the Φ-dependence of the compressibility.[28] For the studied sample at $\Phi = 30\%$, the mean interparticle distance is comparable to the size of the effective spheres. They are slightly interpenetrated, giving rise to the glassy behavior of the sample.

When applying a magnetic field, the magnetic dipoles align along **H**. Since interparticle repulsion is dominant, the bodies of the NPs remain well separated and there is no signs of self-assembled anisotropic structures. However the interaction potential becomes slightly anisotropic, inducing a slight anisotropic structure (see the anisotropy of the scattered intensity and $S(Q)$ in Fig. 1). The largest anisotropy is observed on the scale of the interparticle distance, *i.e.* on the peak of $S(Q)$. It is quantified by its maximum S_{max} and shows a similar behavior to ferrofluids in the fluid phase. S_{max} increases in the perpendicular direction, due to the increase of interparticle repulsion under magnetic dipolar interaction. S_{max} decreases in the parallel direction due to the effect of dipolar interaction combined with NPs fluctuations along the field direction.[23] Only a small shift

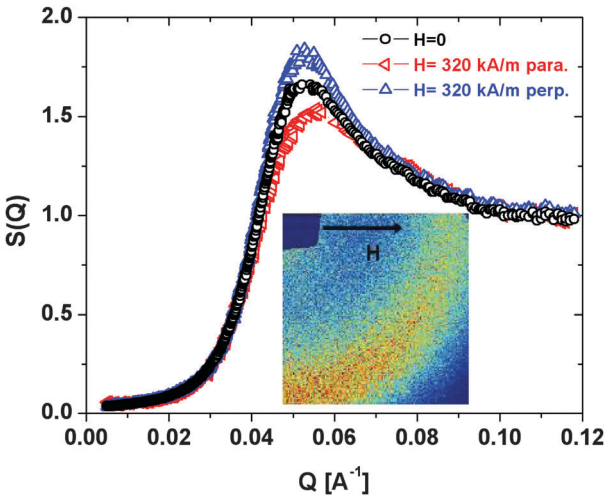

Fig. 1 Static structure factor $S(Q)$ obtained by SAXS, for **H** = 0 (circles) and H = 320 kA m^{-1} (triangles). Inset: speckle pattern of a quadrant of the scattered intensity for H = 320 kA m^{-1}. The direction of **H** is indicated by the arrow.

of its position Q_{max} occurs while, on larger scales, the compressibility remains almost isotropic.

We already have investigated the anisotropy of the local structure under-field over the whole Φ range in a recent paper,[28] showing that the NPs are trapped in an anisotropic cage formed by their first neighbors. The structural anisotropy is interpreted by a model of magnetostriction, relying on the under-field deformation of anisotropic cages formed by neighboring NPs. This model is based on the elastic deformation of the cage at constant volume under the applied field and describes very well the Q_{max} and S_{max} anisotropies. It provides a measure of the elastic modulus of the magnetic fluid. In this model the anisotropy of the cage is expressed as:[28]

$$\alpha = \frac{d_\perp - d_\parallel}{d_0} = \frac{9}{4\pi}\frac{\mu_0 {M_{MF}}^2(H)\sigma_H{}^2}{k_B T} \qquad (1)$$

where $d_\perp$ (resp. $d_\parallel$) is the size of the cage in the perpendicular (resp. parallel) direction of the field, d_0 its dimension in absence of field, $M_{MF}(H)$ the magnetization of the magnetic fluid and ${\sigma_H}^2$ the mean squared displacement of the NP, taken isotropic in the model of ref. 28. Fitting the experimental data in the framework of this model, provides a modest anisotropy of the cage $\alpha \approx 8\%$.[28] It however means that the interpenetration of the effective spheres under an **H** field is slightly anisotropic. This could have dynamical consequences as the experimental broadening of $S(Q)$ in the parallel direction suggest ${\sigma_H}^2$ to be slightly anisotropic with $\sigma_\perp < \sigma_\parallel$ (see Fig. 9 in ref. 28). Only XPCS dynamical study can shed some light on this question.

4 Translational dynamics of the nanoparticles

From the XPCS measurements we compute the degree of temporal correlation between two speckle patterns, separated by a lag-time τ, at a time t:[13,29]

$$c_I(Q,\tau,t) = \frac{\langle I_p(Q,t) I_p(Q,t+\tau)\rangle_Q}{\langle I_p(Q,t)\rangle_Q \langle I_p(Q,t+\tau)\rangle_Q} - 1 \qquad (2)$$

where $I_p(Q,t)$ is the intensity at pixel p and time t, $\langle\cdots\rangle_Q$ denotes an ensemble average over pixels in a ring of iso-wavevectors Q (for isotropic patterns). Under field, the scattering pattern is anisotropic, thus the average in eqn (2) is restricted to the same angular sectors as for $S(q)$ along and perpendicular to **H**. We also observe that for zero field (*i.e.* in the isotropic case) this average on a reduced azimutal area does not modify the obtained results. The time average of c_I provides the usual intensity autocorrelation function:

$$g^{(2)}(Q,\tau,t_w) = \langle c_I(Q,t,\tau)\rangle_{t_w} + 1 \qquad (3)$$

where $\langle\ldots\rangle_{t_w}$ denote a time average (over 200 frames) centered on age t_w.† In addition, we compute at all accessible Q's the temporal variance of c_I, normalized as described in ref. 24 and 30 $\chi(\tau) = \mathrm{var}[c_I(Q,\tau,t)]/\langle c_I(Q,\tau,t)\rangle$. It is related to the dynamical susceptibility χ_4[3,5,9,30] and provides information on the heterogeneous nature of the dynamics.

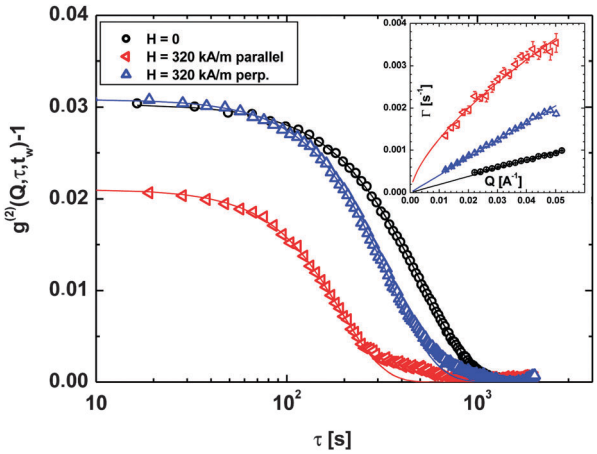

Fig. 2 $g^{(2)}(Q,\tau,t_w)$ as a function of τ for Q = 0.048 Å^{-1} and t_w = 5622 s. Lines are compressed exponential fits, $g^{(2)} - 1 \propto \exp[-2(\Gamma t)^\beta]$, with $\beta > 1$. Inset: $\Gamma(Q)$, at t_w = 5622 s. Lines are linear fits for H = 0 and in the parallel direction. For the perpendicular direction, the line is a power law fit $\Gamma = 0.025\ Q^{0.66}$.

The $g^{(2)}$'s at Q = 0.048 Å^{-1} and $t_w = 5622 \pm 375$ s, are plotted in Fig. 2 with and without applied field. The observed decay of $g^{(2)}$ is faster when a field is applied. This effect is stronger along the field direction and associated to a smaller non-ergodicity factor (defined here as $g^{(2)}$ at short τ). These features are observed on all probed Q's and t_w's. The $g^{(2)}$'s can be fitted by compressed exponentials[26] and the inverse characteristic time $\Gamma = {\tau_c}^{-1}$ increases linearly with Q for **H** = 0, as observed on many glassy systems.[30] This is referred to as a ballistic behavior and is only observed in the perpendicular direction in the presence of a magnetic field, as observed in the inset of Fig. 2. In the parallel direction, we observe a non linear dispersion $\Gamma(Q)$. This behavior is reminiscent of de Gennes' narrowing, occurring at Q's close to Q_{max}.[31] This non linearity is also comparable to the superballistic behavior evidenced in ref. 32 with $\Gamma \sim Q^{2/3}$ (inset of Fig. 2). However, given our limited Q range we cannot conclude on the origin of this non linearity. Interestingly, such an anomalous dynamics in the direction of the field is reported in theoretical works that consider the anisotropic dynamics of a single particle either driven by a constant force in a glass-forming system[21] or evolving in a biased potential energy landscape.[22] In our system, the application of a field tends to reduce the energy barriers in the direction of **H**, due to dipolar interactions. This biased and anisotropic energy landscape could thus explain the anomalous $\tau(Q)$ relationship in the parallel direction. If so, one would expect large temporal fluctuations of the dynamics in the parallel direction and thus a possible signature of it in $\chi(\tau)$.

The dynamical susceptibility $\chi(\tau)$ without and with magnetic field is plotted in Fig. 3 for Q = 0.048 Å^{-1}. When a dynamical cluster of NPs relaxes in the sample, it induces a drop of the correlator c_I. $\chi(\tau)$ is then maximum on the timescale of these relaxation processes and its maximum χ^* measures the degree of cooperativity of the dynamics.[24,30] Therefore the peak position

† For the present sample, the age dependence of the dynamics is complex as two aging regimes are observed[26] for H = 0 and an anisotropic aging is observed under field (data not shown). The c_I's are analyzed here in the slow aging regime of ref. 26.

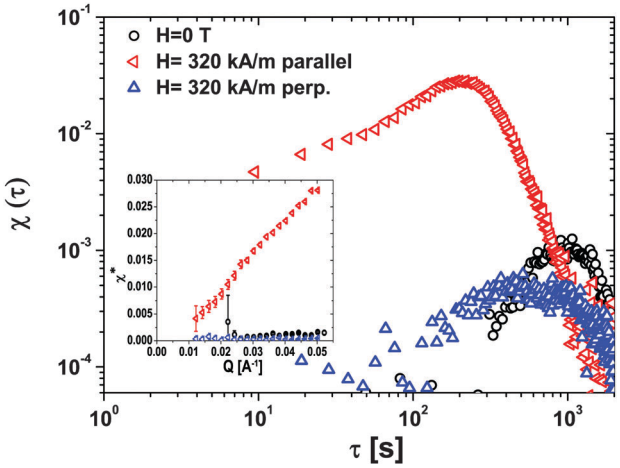

Fig. 3 $\chi(\tau)$ at Q = 0.048 Å^{-1}, at 0 and 320 kA m^{-1}, parallel or perpendicular to **H** direction. Inset: maximum of $\chi(\tau)$ as a function of Q.

corresponds to the characteristic time τ_c of $g^{(2)}$ and reproduces the anisotropy seen in Fig. 2. The χ^* values are also highly anisotropic being almost two orders of magnitude larger in the parallel direction than in perpendicular one. Assuming that χ^* is proportional to the cube of the size of the dynamic clusters,[30] it gives dynamically correlated clusters elongated along **H** with an anisotropy ratio of the order of 4 to 5.

The Q-dependence of χ^* is presented in the inset of Fig. 3. When **H** = 0, χ^* is nearly constant with Q, as in ref. 24. Under field, χ^* in the perpendicular direction is smaller than for **H** = 0, and characterizing its Q-dependence is difficult. In the parallel direction χ^* grows linearly with Q, providing evidence that the cooperative process takes place on local length-scales. The faster dynamics in the parallel direction appears to be driven by cooperative events at short time and lengthscales.

5 Discussion

The application of a magnetic field on this repulsive and magnetic colloidal glass has both structural and dynamical consequences. We can first interpret the field effect as a geometrical perturbation of the **H** = 0 situation. Since the magnetic dipolar interactions reduce the repulsion between NP's in the direction of **H**, the system can still be considered as interpenetrated effective spheres, but trapped in anisotropic cages and coupled to both an external magnetic field and to a thermal bath. There is a growing interest to consider the dynamics of anisotropic systems, such as hard ellipsoids[33] or dumbbells.[34] For instance, Zheng *et al.* measure the dynamics of concentrated hard ellipsoids dispersions[33] and show that at a given Φ, the cooperativity of the translational dynamics is anisotropic. However, our situation is different in essence, since the anisotropy of the interaction is due to a global coupling to the field rather than set by a local anisotropic range of interaction as for hard ellipsoids. The coupling to the field modulates the local fluctuations of position of the NPs. These fluctuations are anisotropic, being larger along **H** and are hindered by the cages inside which the NPs are confined. They are then the "motors" of coherent fluctuations of adjacent cages in the **H** direction, increasing the cooperativity and decreasing the non-ergodicity factor on the scale of a few interparticle distances.

Consequently, in presence of the field, the energetic landscape of the system is anisotropic and due to reduced repulsions along the **H** direction, the time scale of barrier-crossing is lower and the relaxation is faster. In qualitative agreement with ref. 21 and 22 we report an anomalous dynamics $\tau(Q)$ in the parallel direction to the field, together with highly cooperative dynamics, due to the field-driven fluctuations of position of the NPs. This enhanced cooperativity in the direction of reduced repulsion can be compared to simulations of hard sphere where the interaction potential is tuned.[35,36] By computing numerically χ_4 in (isotropic) colloidal hard sphere glasses and gels Coniglio *et al.* show that in glasses χ_4 is peaked in time, expressing the transient nature of the cooperative processes, whereas in gels χ_4 reaches a plateau, expressing the persistent presence of large relaxing clusters. In our case, in the parallel direction to **H**, the system is not made of permanent structures at contact, the rearrangements of which lead to a giant cooperativity on long timescales. On the contrary, the $\chi(\tau)$ we report on seems to plateau at short times, the dynamical fluctuations being driven by short timescales field induced fluctuations.

In the perpendicular direction, the dynamics is slower and less cooperative. This is in contradiction with the picture of growing cooperative domains, used to explain the slowing down of the dynamics in glasses. However, the reduced particle displacements in very dense suspensions tends to decrease χ^* despite of the growing size of the cooperative clusters.[30] It leads to a non-monotonic Φ-dependence of χ^*, with a maximum at a volume fraction Φ_c and a decay for higher Φ's. A similar scenario could take place here, supported by the observed reduced mean squared displacements in the perpendicular direction $\sigma_\perp < \sigma_0 < \sigma_\parallel$,[28] along with the widening of $S(Q)$ around Q_{max} in the parallel direction.

Another striking result is the observation of a quasi-linear increase of the dynamical susceptibility peak χ^* with Q in the parallel direction (inset of Fig. 3). This latter is in qualitative agreement with a scaling argument developed by Trappe *et al.* In ref. 13 the authors predict the Q dependence of χ^*, showing that $\chi^* \sim (N_{blob}N_{ev})^{-1}$, with N_{blob} the number of dynamically correlated "blobs" in the scattering volume and N_{ev} the number of dynamical events needed, at a given location, to relax the local contribution to the correlation function. This latter being proportional to time, one expects $N_{ev} \sim \tau_c \sim Q^{-\alpha}$. On the other hand, in ref. 13 the authors argue that it is reasonable (in their isotropic system) to expect that N_{blob} increases with Q (the cooperativity involving less particles at smaller lengthscales), with a saturation at high Q. In summary χ^* can present complex non monotonic Q variations, with $\chi^* \sim Q^{+\alpha}$ in the low Q limit, *i.e.* $Q < Q_{max}$. This asymptotic limit is in qualitative agreement with our reported results. In the parallel direction to the field, we indeed observe an increase of χ^* with Q, for $Q < Q_{max}$, bringing evidence that the cooperative processes take place at small lengthscales.

On the basis of this model, we extract the number of correlated blobs N_{blob} in our anisotropic system. We present on Fig. 4 the ratio $\chi^*/\Gamma \sim {N_{blob}}^{-1}$ as a function of Q. While in absence of field ${N_{blob}}^{-1}$ is roughly Q independent, it becomes

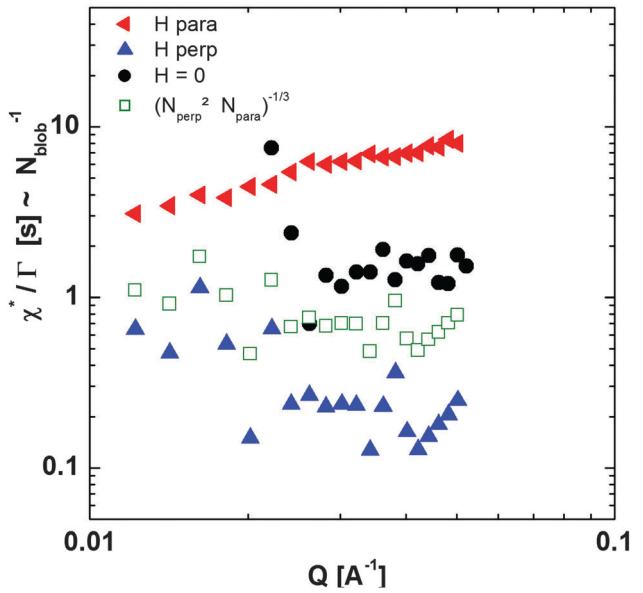

Fig. 4 $\chi^*/\Gamma \sim N_{blob}{}^{-1}$ as a function of Q in zero field (circles) and 320 kA m^{-1}, parallel (horizontal triangles) or perpendicular (vertical triangles) to **H** direction. The square symbols represent $((\chi_{\parallel}{}^*/\Gamma_{\parallel})(\chi_{\perp}{}^*/\Gamma_{\perp})^2)^{1/3}$ as a function of Q.

highly anisotropic under field. $N_{blob}{}^{-1}$ spans over almost two orders of magnitudes at high Q's, between the parallel and perpendicular directions to the field. In the parallel direction, the number of correlated blobs $N_{blob\parallel}$ decreases with Q – another indication that the cooperative processes take place at small lengthscales. In the perpendicular direction the number of correlated blobs $N_{blob\perp}$ is larger than in the parallel direction over all the probed Q range and increases with Q. Since magnetization inhomogeneities are the probable source of these under field anisotropic fluctuations, we can understand why the fluctuations are more limited in the perpendicular direction, for which magnetization inhomogeneities are weaker. Last, let us notice that $(N_{blob\parallel}N_{blob\perp}{}^2)^{-1/3}$ (square symbols on Fig. 4) is roughly Q independent and close to its value in zero field. This means that the number of correlated particles under field is anisotropic but that the overall number is conserved with respect to the zero field situation.

To conclude, let us notice that anisotropic cooperative processes have already been reported in hard sphere colloidal glasses undergoing a macroscopic shear.[17,18] However, a special interest of the reported field induced cooperativity is that it arises from a global perturbation of the interaction potential leading to a presumably spatially uniform perturbation of the dynamics. This is in contrast with macroscopic shear which leads to shear banding at high shear rates as in ref. 18 and thus to an heterogeneous spatial distribution of the cooperative domains.

6 Conclusion

In conclusion, using XPCS experiments, we have probed the translational dynamics of a repulsive colloidal glass made of magnetic nanoparticles. Under the application of a magnetic field the dynamics of the system is faster than in zero field. The dynamics is anisotropic, being faster along the field than in the perpendicular direction. In the parallel direction an anomalous dynamics $\tau(Q)$ is observed, associated to a huge increase of the dynamical susceptibility, in qualitative agreement with biased trap models[22] and recent numerical simulations.[21] All these features are qualitatively recovered at any ages of the sample. The field intensity could thus be potentially used as a way to tune and orientate the dynamical cooperativity. This system has through the magnetic field a powerful control parameter. Conjugating experiments on glassy samples at various Φ (even if a limited range is accessible) probed at various H is a promising route to understand how the dynamical heterogeneities vary at the approach of the glass transition. In particular, probing the complete **H** dependence of the dynamical susceptibility should bring interesting results, including a linear regime at low fields (for which $M \sim H$) and the transition to a nonlinear response regime at higher fields.

Acknowledgements

The authors acknowledge the whole team of the ID02 beamline of ESRF for their help in the small angle X-ray scattering (SAXS) measurements and D. Talbot for the synthesis of ionic ferrofluids.

References

1 F. H. Stillinger and P. G. Debenedetti, *Annu. Rev. Condens. Matter Phys.*, 2013, **4**, 263–285.
2 L. Berthier and G. Biroli, *Rev. Mod. Phys.*, 2011, **83**, 587–645.
3 G. Biroli and J. P. Garrahan, *J. Chem. Phys.*, 2013, **138**, 12A301.
4 P. Schall, D. Weitz and F. Spaepen, *Science*, 2007, **318**, 1895.
5 L. Berthier, G. Biroli, J.-P. Bouchaud, W. Kob, K. Miyazaki and D. R. Reichman, *J. Chem. Phys.*, 2007, **126**, 184503.
6 G. Brambilla, D. E. Masri, M. Pierno, L. Berthier, L. Cipelletti, G. Petekidis and A. B. Schofield, *Phys. Rev. Lett.*, 2009, **102**, 085703.
7 T. Abete, A. de Candia, E. D. Gado, A. Fierro and A. Coniglio, *Phys. Rev. E: Stat., Nonlinear, Soft Matter Phys.*, 2008, **78**, 041404.
8 C. Brun, F. Ladieu, D. L'Hôte, G. Biroli and J.-P. Bouchaud, *Phys. Rev. Lett.*, 2012, **109**, 175702.
9 C. Crauste-Thibierge, C. Brun, F. Ladieu, D. L'Hôte, G. Biroli and J.-P. Bouchaud, *Phys. Rev. Lett.*, 2010, **104**, 165703.
10 L. Berthierl, G. Biroli, J.-P. Bouchaud, L. Cipelletti, D. E. Masri, D. L'Hôte, F. Ladieu and M. Pierno, *Science*, 2005, **310**, 1797.
11 F. Bert, V. Dupuis, E. Vincent, J. Hammann and J.-P. Bouchaud, *Phys. Rev. Lett.*, 2004, **92**, 167203.
12 R. Zargar, B. Nienhuis, P. Schall and D. Bonn, *Phys. Rev. Lett.*, 2013, **110**, 258301.
13 V. Trappe, E. Pitard, L. Ramos, A. Robert, H. Bissig and L. Cipelletti, *Phys. Rev. E: Stat., Nonlinear, Soft Matter Phys.*, 2007, **76**, 051404.
14 A. Duri, D. Sessoms, V. Trappe and L. Cipelletti, *Phys. Rev. Lett.*, 2009, **102**, 085702.

15 M. D. Haw, *Philos. Trans. R. Soc., A*, 2009, **367**, 5167.
16 R. Yamamoto and A. Onuki, *Phys. Rev. E: Stat. Phys., Plasmas, Fluids, Relat. Interdiscip. Top.*, 1998, **58**, 3515.
17 A. Furukawa, *et al.*, *Phys. Rev. Lett.*, 2009, **102**, 016001.
18 V. Chikkadi, *et al.*, *Phys. Rev. Lett.*, 2011, **107**, 198303.
19 R. Candelier and O. Dauchot, *Phys. Rev. Lett.*, 2009, **103**, 128001.
20 L. B. K. Martens and J.-L. Barrat, *Phys. Rev. Lett.*, 2011, **106**, 156001.
21 D. Winter, J. Horbach, P. Virnau and K. Binder, *Phys. Rev. Lett.*, 2012, **108**, 028303.
22 J.-P. Bouchaud and A. Georges, *Phys. Rep.*, 1990, **195**, 127.
23 G. Mériguet, F. Cousin, E. Dubois, F. Boué, A. Cebers, B. Farago and R. Perzynski, *J. Phys. Chem. B*, 2006, **110**, 4378.
24 E. Wandersman, E. Dubois, V. Dupuis, A. Robert and R. Perzynski, *J. Phys.: Condens. Matter*, 2008, **20**, 204124.
25 G. Mériguet, M. Jardat and P. Turq, *J. Chem. Phys.*, 2005, **123**, 144915.
26 A. Robert, E. Wandersman, E. Dubois, V. Dupuis and R. Perzynski, *EPL*, 2006, **75**, 764.
27 E. Wandersman, V. Dupuis, E. Dubois and R. Perzynski, *Phys. Rev. E: Stat., Nonlinear, Soft Matter Phys.*, 2009, **79**, 7575.
28 E. Wandersman, A. Cebers, E. Dubois, G. Mériguet, A. Robert and R. Perzynski, *Soft Matter*, 2013, **9**, 11480.
29 A. Duri and L. Cipelletti, *EPL*, 2006, **76**, 972.
30 P. Ballesta, A. Duri and L. Cipelletti, *Nat. Phys.*, 2008, **4**, 2008.
31 C. Caronna, Y. Chushkin, A. Madsen and A. Cupane, *Phys. Rev. Lett.*, 2008, **100**, 055702.
32 J. Duplat, S. Kheifets, T. Li, M. Raizen and E. Villermaux, *Phys. Rev. E: Stat., Nonlinear, Soft Matter Phys.*, 2013, **87**, 020105(R).
33 Z. Zheng, F. Wang and Y. Han, *Phys. Rev. Lett.*, 2011, **107**, 065702.
34 S.-H. Chong and W. Kob, *Phys. Rev. Lett.*, 2009, **102**, 025702.
35 A. Coniglio, T. Abete, A. de Candia, E. D. Gado and A. Fierro, *J. Phys.: Condens. Matter*, 2007, **19**, 205103.
36 A. Fierro, T. Abete, A. de Candia, E. D. Gado and A. Coniglio, *J. Phys.: Condens. Matter*, 2009, **21**, 504110.

